Multi-objective optimization of the process parameters for friction welding of dissimilar metals

Radosław Winiczenko[1,*], *Andrzej* Sibicki[2] , *Paweł* Skoczylas[3], and *Jędrzej* Trajer[1]

[1]Faculty of Production Engineering, Warsaw University of Life Sciences, Nowoursynowska 166, 02-787, Warsaw, Poland
[2] Faculty of Mechanical Engineering, University of Science and Technology, Al. prof. S. Kaliskiego 7, 85-796, Bydgoszcz, Poland
[3] Faculty of Production Engineering, Warsaw University of Technology, Narbutta 85, 02-524, Warsaw, Poland

Abstract. This paper presents a multi-objective optimization method for optimizing the process parameters during friction welding of dissimilar metals. The proposed method combines the response surface methodology (RSM) with an a genetic algorithm (GA) method. Ultimate tensile strength (UTS), flash diameter and the heat affected zone (HAZ) width of friction welded nodular cast iron with low carbon steel joints were investigated considering the following process parameters: friction pressure (FP), friction time (FT) and upsetting pressure (UP). Mathematical models were developed and the responses were adequately predicted. Direct and interaction effects of process parameters on responses were studied by plotting graphs. In the case of UTS, FT has high significance followed by: FP and UP. Friction time has high significance on the flash diameter of nodular cast iron followed by UP and FP. However in the case of the low carbon steel flash diameter, UP has high significance followed by FT and FP. In the case of the HAZ width for nodular cast iron and low carbon steel side, friction time has high significance followed by UP and FT. Multi-objective optimization for maximizing the tensile strength and minimizing the flash diameter and the HAZ width was carried out using mathematical model.

1 Introduction

Friction rotary welding (FRW) is a method of joining materials which can be welded with difficulty [1]. Thus, ductile iron can be welded and also joined to other materials such as steels with high alloy-content by FRW [2, 3]. FRW of ductile iron is not possible because graphite acts as a lubricant and prevents the generation of heat sufficient for joining [4, 5]. Ductile iron-steel welded joints are particularly difficult to produce since carburization takes place on the low carbon side with carbide formation. On the other hand, FRW is a

* Corresponding author: radoslaw_winiczenko@sggw.pl

method of welding which has recently been used to connect grey cast iron with both the flake graphite [6, 7] and the nodular graphite [8-10].

The FRW process parameters such as: rotational speed, pressure at the weld interface, and heating time are the variables that must be considered in direct drive friction welding [11, 12]. To produce a good quality joint it is important to set up proper welding parameters. Thus, identifying the suitable combinations of the process input parameters to produce the desired output requires many experiments, making this process time consuming and costly [13]. In the welding procedures various optimization methods can be applied to define the desired output variables through developing mathematical models to specify the relationship between the input parameters and output variables. In the last two decades, design of experiment (DOE) techniques have been used to carry out such optimization [14-15]. The various mathematical models can be built, which can adequately predict the relation between input process parameters and the responses.

Paventhan et al. [16, 17] used the RSM to optimize the friction welding parameters for joining aluminium alloy and stainless steel. Sathiya et al. [18, 19] have done the optimization of friction welding parameters using simulated annealing and evolutionary computational techniques. Yamaguchi et al. [20] have investigated the friction welding process of 5056 aluminium alloy using RSM. Ozdemir et al. [21] studied the influence of the rotational speed on the properties of friction welded AISI-304L to 4340 steel. Hakan et al. [22] studied the properties of friction welded MA956 iron based super alloy in order to select the optimal friction pressure. Koichi et al. [23] have studied the combination of welding conditions that produce maximum notched tensile strength of friction welded joints of S45C carbon steel using RSM. Udayakumar et al [24, 25] conducted optimization for maximizing the impact strength and minimizing the corrosion resistance using intelligent hybrid method.

The presented knowledge on friction welding of ductile iron is focused on the structural and mechanical properties, phase formation and tensile strength evolution. These all investigations were carried out on trial and other basis to attain optimum welding conditions. The combined effects of process parameters on multi responses like tensile strength, flash diameter and the HAZ width in ductile iron with low carbon steel joints are hitherto not reported. Only other materials such as stainless steel, aluminium alloys, magnesium or titanium alloys were considered by many researchers. The main reason for this situation can be fact that ductile iron is generally considered as a material difficult to weld.

The first aim is to employ RSM to develop empirical relationships relating the friction welding input parameters (friction pressure, friction time and upsetting pressure and five output responses (i.e. tensile strength, flash diameter for ductile iron and low carbon steel and the ductile iron and steel HAZ width). The second aim is to find the *Pareto*-optimal parameters welding combination that would maximize both the tensile strength and minimize the flashes and the HAZ width for friction welding joints.

2 Experimental procedure

The following independently controllable process parameters were indentified to carry out the experiments: friction pressure (F), friction time (T) and upsetting pressure (U). Other friction welding parameters like rotational speed and upsetting time could be set at any desired level within the range of the machine setting. In this study constant rotational speed (1450 rpm) and upsetting time (3s) are used. The working ranges of all selected parameters were fixed by conducting trial runs. This was carried out by varying one of the parameters while keeping the rest of them at constant values. The working range of each process welding parameters was decided upon by inspecting the weld for a smooth appearance

without any visible defects. The upper and lower limits with different levels of the identified process parameters are presented in Table 1.

Table 1. Process variables and their bounds.

#	Parameter	Notation	Unit	Factor levels		
				-1	0	1
1	Friction pressure	F	MPa	35	41	48
2	Friction time	T	s	40	65	90
3	Upsetting pressure	U	MPa	86	118	150

The selected design matrix (see Table 2) is a central composite face centered factorial design consisting of 20 sets of coded conditions [26, 27]. It comprises a full replication of 23 (8) factorial design plus six center points and six star points. All friction welding variables at the intermediate level (0) constitue the center points and the combinations of each of the welding variables at either their lowest (-1) level or highest (+1) level with the other two variables at the intermediate levels constitue the star points. Thus the 20 experimental runs allowed the estimation of the linear, quadratic and two way interactive effects of the friction welding parameters. The results of RSM are given in Table 2.

Table 2. Design matrix and experimental design.

No.	Coded value			Actual value			Responses				
#	F	T	U	F	T	U	TS	DFDI	DFLCS	HAZ DI	HAZ LCS
1	-1	-1	-1	35	40	86	304	22	19	23	24
2	1	-1	-1	48	40	86	348	24	23	24	24
3	-1	1	-1	35	90	86	414	28	24	28	33
4	1	1	-1	48	90	86	496	32	25	86	32
5	-1	-1	1	35	40	150	118	17	24	21	22
6	1	-1	1	48	40	150	383	20	26	21	22
7	-1	1	1	35	90	150	306	25	28	86	30
8	1	1	1	48	90	150	311	28	30	86	30
9	-1	0	0	35	65	118	283	23	24	26	86
10	1	0	0	48	65	118	297	26	25	25	86
35	0	-1	0	41	40	118	343	21	22	22	23
12	0	1	0	41	90	118	363	29	86	86	31
41	0	0	-1	41	65	86	290	86	22	86	29
14	0	0	1	41	65	150	303	23	86	24	25
48	0	0	0	41	65	118	289	25	24	25	86
16	0	0	0	41	65	118	290	25	24	25	86
17	0	0	0	41	65	118	291	25	24	25	86
18	0	0	0	41	65	118	287	25	24	25	86
19	0	0	0	41	65	118	286	25	24	25	86
20	0	0	0	41	65	118	292	25	24	25	86

The experimental was conducted as per the design matrix using a continuous direct drive friction welding machine type of ZT4-13. The friction welding was done on (ASTM 80-55-06) ductile iron with (AISI 1020) low carbon steel rods size 20 mm diameters and 100 mm length. Tensile strength test was conducted for 20 friction welded samples and the

tensile strength value was recorded. All of the friction welds were tested at room temperature using an Instron tensile test machine. The results obtained from the testing with welding parameters are shown in Table 2. In the present work the flash diameter was measured after friction welding. The flash features are significant factors which are to be considered in minimizing material loss. The establish color etching procedure for the materials was employed to identify different regions of the weldment. An optical microscope (NEOPHOT-32) was used. With the help of built-in linear measuring devices in the microscope that had an accuracy of 0.001 mm, dimension (width) of the HAZ was measured.

3 Development of empirical relationships

In this study, the response functions of the ductile iron-low carbon steel joint: tensile strength (TS), diameter of flash (DFLASH) and width of HAZ (WHAZ), are functions of friction pressure (F), friction time (T) and upsetting pressure (U), and it can be expressed as:

$$Y\ (TS, DFLASH, WHAZ) = f\ (F, T, U) \tag{1}$$

The mathematical models to establish the relationships between input and output parameters were developed using Design-Expert 7.0 (Statease Inc., USA) software at a confidence level of 95%. Tensile strength and flash diameter where expressed as a non-linear function of process parameters. The second order polynomial equation that represent the response surface 'Y' is:

$$Y = b_0 + \sum b_i x_i + \sum b_{ii} x_i^2 + \sum b_{ii} x_i x_j + e_r \tag{2}$$

Considering three parameters, the selected polynomial could be expressed as:

$$Y = b_0 + b_1(F) + b_2(T) + b_3(U) + b_{12}(FT) + b_{13}(FU) + b_{23}(TU) + b_{11}(F^2) + (T^2) + b_{33}(U^2) \tag{3}$$

where b_0 is the average of responses and bi and b_{ij} are the response coefficients that depend on response coefficient that depend on respective main and interaction effects of the parameters. In this work, central composite design which accurately fits the second order response surface was used. The value of the coefficient was calculated by applying central composite design using Design-Expert Software [20]. The significance of each of the model terms was checked using p values. The value of p less than 0.05 indicate that the model terms are significant. The values greater than 0.05 indicate that the model terms are not significant. Values greater than 0.1 indicate the model terms are not significant. Insignificant model terms that are not satisfying the above said criteria have been eliminated by backward elimination regression method, without affecting much of the accuracy of the model. In the tensile strength model, the model terms FU, F^2 and U^2 were found insignificant and eliminated. In the case of flash of ductile iron, the model terms FU, T^2 and U^2 were found insignificant and eliminated (see Table 3). In the case of carbon steel flash, the all model terms were found significant.

Table 3. ANOVA results for tensile strength, flash diameter and the HAZ width.

	Tensile strength		Flash diameter		HAZ width	
Source			ductile iron	steel	ductile iron	steel
	F-value	Prob > *F*	*F*-value	*F*-Value	*F*-value	*F*-value
Model	44	< 0.0001	387	79	60	533
F	14	0.0036	375	24	0.26	0.86
T	26	0.0005	2407	97	160	1454
U	8.8	0.0141	667	117	21	146
F·T	8.2	0.0166	8.33	-	-	-
F·U	2.8	0.1223	0.000	-	-	-
T·U	146.7	< 0.0001	8.33	-	-	-
F^2	0.15	0.7037	11.46	-	-	-
T^2	83.56	< 0.0001	0.000	-	-	-
U^2	1.67	0.2247	0.000	-	-	-
Coefficient	R^2	0.97	0.99	0.94	0.92	0.99
Adjusted	R^2	0.95	0.99	0.92	0.90	0.98
Predicted	R^2	0.74	0.94	0.88	0.84	0.98
Adequate Precision		24.23	84.29	36.21	25.04	72.33

The final mathematical models were constructed using only significant terms, and developed empirical relationship. The equations in terms of coded factors:

$$TS = 288.37 + 14.30\,(F) + 19.30\,(T) - 11.20\,(U) + 12.13\,(FT) - 51.12\,(TU) + 65.82\,(T^2) \quad (4)$$

$$DFLASH_{DI} = 25.00 + 1.50\,(F) + 3.80\,(T) - 2.00\,(U) + 0.25\,(FT) + 0.25\,(TU) + -0.50\,(F^2) \quad (5)$$

$$DFLASH_{LCS} = 24.50 + 1.00\,(F) + 2.00\,(T) + 2.20\,(U) \quad (6)$$

$$WHAZ_{DI} = 24.95 - 0.1\,(F) + 2.5\,(T) - 0.9\,(U) \quad (7)$$

$$WHAZ_{LCS} = 27.05 - 0.1\,(F) + 4.1\,(T) - 1.3\,(U) \quad (8)$$

3.1 Validation of the developed models

The adequacy of the developed relationship was tested using the analysis of variance technique (ANOVA) [27]. In this research, the desired level of confidence was considered to be 95%. The basic adequate ANOVA test results for all responses are presented in Table. 3. The model F values of 44 for tensile strength, 387 and 79 for the flash diameter and 60 and 533 for the HAZ width respectively, imply the models are significant. Coefficient of determination 'R^2' is used to find how close the predicted and experimental values lie. The value of 'R^2' for tensile strength and flash diameter indicate high correlation exists between the experimental and predicted values. The 'Adequate Precision' measures the signal to noise ratio. A ratio greater that 4 is desirable. There is an adequate signal in all models. Each predicted value matches well with its experimental value, as shown in Figs. 1 and 2.

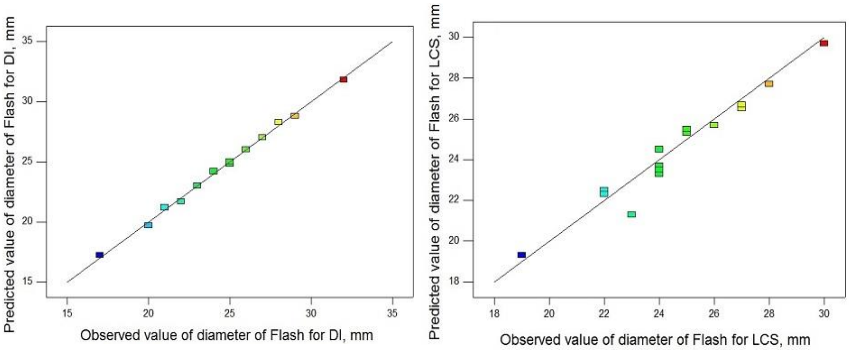

Fig. 1. Predicted value of flash diameter vs. observed value of flash diameter

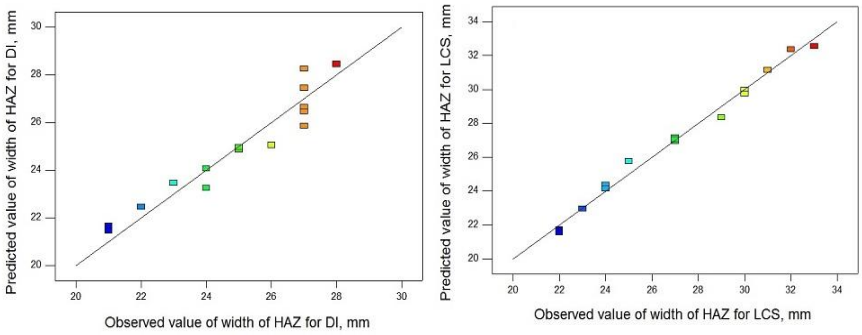

Fig. 2. Predicted value of HAZ width vs. observed value of HAZ width

3.2 Optimization procedure

Optimization toolbox in Matlab 8.0 was used for generating the Pareto front for tensile strength and flash diameter using Multi-objective genetic algorithm (MOGA). MOGA uses a controlled elitist genetic algorithm (a variant of Non-dominated sorting genetic algorithm II (NSGA-II)). An elitist genetic algorithm always favors individuals with better fitness value (rank) [28]. A controlled elitist GA also favors individuals that can help increase the diversity of the population even if they have a lower fitness value. It is important to maintain the diversity of population for convergence to an optimal Pareto front. Diversity is maintained by controlling the elite members of the population as the algorithm progresses. Two options in Matlab Toolbox: Pareto front population fraction (ParetoFraction) and distance measure function (DistanceFcn) control the elitism. "ParetoFraction" limits the number of individuals on the Pareto front (elite members). The distance measure function, helps to maintain diversity on a front by favouring individuals that are relatively far away on the front. The algorithm stops if the spread, a measure of the movement of the Pareto front, is small [27].

A Matlab function was written using the developed RSM models in terms of actual factors. These functions were called as the input for creating a fitness function for the multi-objective optimization problem. The tensile strength to be maximized was negated in the fitness function since algorithm minimizes all the objectives. Experimental ranges were placed as bounds on the three input variables (Table 1). The genetic algorithm MOGA options are shown in Table 4.

Table 4. MOGA genetic algorithm settings.

Population size	30*number of variables
Selection function	Tournament size = 2
Crossover ratio	90 %
Crossover function	Intermediate
Mutation function	Uniform
Mutation ratio	10 %
Pareto front population fraction	0.7
Number generations	200*number of variables

The optimized Pareto front achievement after 120 iterations is shown in Fig. 3. The weighted average change in the fitness function value over 120 generations was used as the criteria for stopping the MOGA algorithm. Each point on the Pareto set is associated with a set of decision variables. These decision process variables are tabulated in Table 5.
To obtain localized optimal operating conditions for tensile strength, flash diameter and of the HAZ width from the Pareto front, the corresponding decision variables were taken from Table 5.

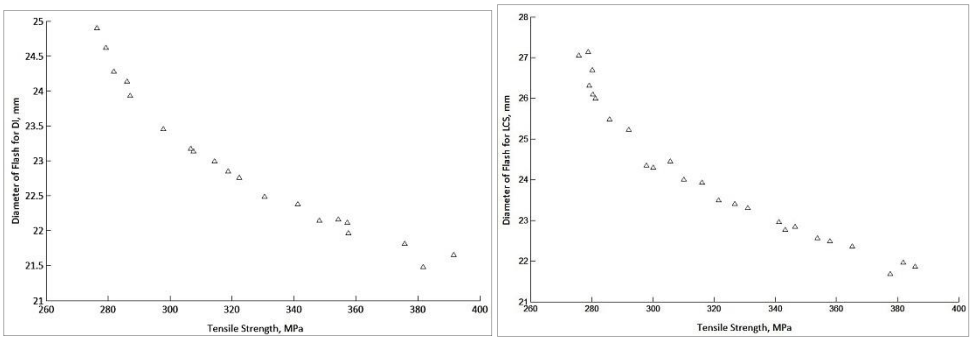

Fig. 3. Pareto front optimal of solutions

Table 5. Process decision variables corresponding to each of the Pareto optimal solutions

Sl. No.	F (MPa)	T (s)	U (MPa)	TS (MPa)	Flash diameter (mm)		HAZ width (mm)	
					DI	LCS	DI	LCS
***1**	**35.06**	**40.02**	**149.68**	**391.67**	**17.02**	**23.70**	**21.75**	**21.65**
2	35.03	40.04	149.68	391.53	17.02	23.70	21.76	21.65
3	45.80	40.01	149.68	381.92	19.39	25.39	21.58	21.48
4	35.03	40.00	144.65	381.68	17.38	23.35	21.96	21.79
5	43.92	42.86	149.33	364.73	19.66	25.30	22.09	21.81
6	35.67	44.61	145.73	354.17	18.19	23.89	22.66	22.21
7	35.67	44.61	145.73	354.17	18.19	23.89	22.66	22.21
8	36.08	42.34	134.14	347.61	18.82	22.98	22.75	22.31
9	38.98	43.25	127.61	332.27	20.28	23.05	23.12	22.54
10	46.50	51.61	148.15	323.35	21.46	26.32	23.54	22.67
11	39.87	52.57	147.36	315.92	20.54	25.30	23.83	22.90
12	35.03	40.00	85.99	297.84	21.59	19.30	24.35	23.45
13	39.17	42.19	87.64	297.22	23.02	20.24	24.58	23.56
14	41.66	54.38	124.39	294.93	22.80	24.14	25.04	23.70
15	39.68	47.89	89.01	288.99	23.84	20.87	25.45	24.08
16	35.03	48.49	90.99	282.49	22.34	20.33	25.54	24.16
17	36.21	49.87	90.51	281.96	22.97	20.59	25.77	24.29
18	35.76	52.43	86.78	278.86	23.41	20.47	26.34	24.66
19	35.03	54.08	86.02	277.41	23.41	20.43	26.66	24.86
20	35.03	54.21	86.94	277.40	23.37	20.50	26.64	24.84

The nondominate optimal points, resulted from multi-objective genetic algorithms, gave insight regarding the optimal operating conditions of the process [27]. These set of solutions can be evaluated for trade off depending on the application considering the tensile strength, flash diameter and the HAZ width of the weld. Further three validation experiments were performed and the response of both the models was found in agreement with the experimental results.

4 Results and discussion

4.1 Direct effect of process parameters

Direct effect of process parameters on each of the responses have been found from the developed mathematical models. The variation of the responses with respect to the friction pressure, friction time and upsetting pressure were plotted by keeping two parameters constant at their central level and varying the third within the upper and lower bounds. The individual variations of the responses with actual welding parameters are presented in Figs. 4-5.

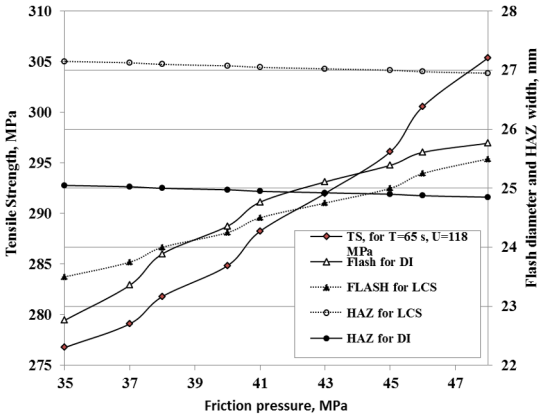

Fig. 4. Effect of friction pressure on tensile strength, flash diameter and the HAZ width

Figure 4 shows the effect of friction pressure on tensile strength, flash diameter and the HAZ width. It is observed that tensile strength and flash diameter increase with an increase in friction pressure. It is also observed that there is a sudeden step up in width of the HAZ as friction pressure changes from 35 to 48 MPa. Friction pressure and friction time have a positive effect on tensile strength. As friction pressure and friction time increases the tensile strength increases. However, initially the tensile strength decreases as friction time increase from 40 to 60s, reaches a minimum and then increases (see Fig. 5). The flash diameter and HAZ width also increase as friction time increases. Upsetting pressure has a negative effect on tensile strength. As upsetting pressure increases the tensile strength decreases.

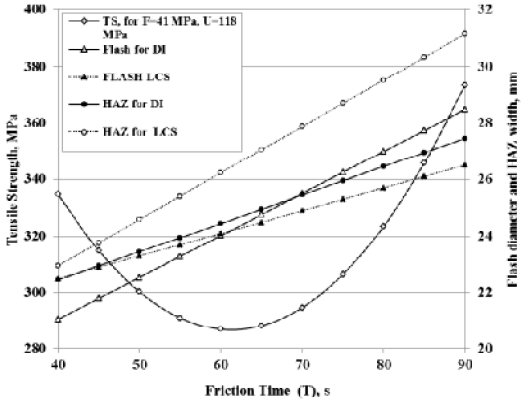

Fig. 5. Effect of friction time on tensile strength, flash diameter and the HAZ width

4.2. Interaction effects of process parameters

The interaction effects of process parameters on tensile strength, flash diameter and HAZ width have been found from the developed mathematical models, which are shown in Figs. 6-8. Fig. 6 shows the interaction effects of friction pressure and friction time on tensile

strength. It is evident that the decreasing trend of tensile strength flattens as friction time changes from 40 to 50 s. As friction time proceeds, tensile strength shows an increasing trend as friction pressure increases. It is observed that there is a sudden increase in tensile strength as friction time changes from 60 to 90 s.

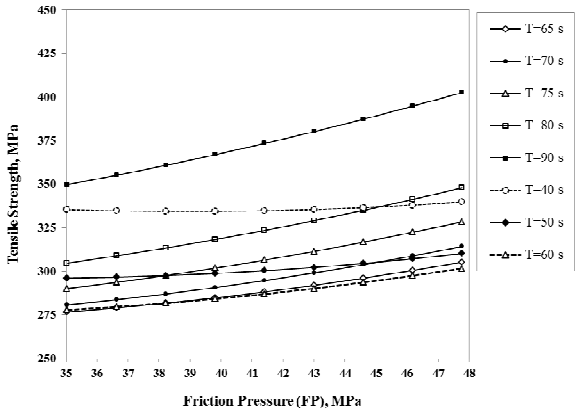

Fig. 6. Effect of friction pressure and friction time on tensile strength

Figure 7 shows the interaction between upsetting pressure and friction pressure on tensile strength. It is clear that, the curves show the same trend as upsetting pressure increases. Tensile strength slowly decreases as friction pressure decreases.

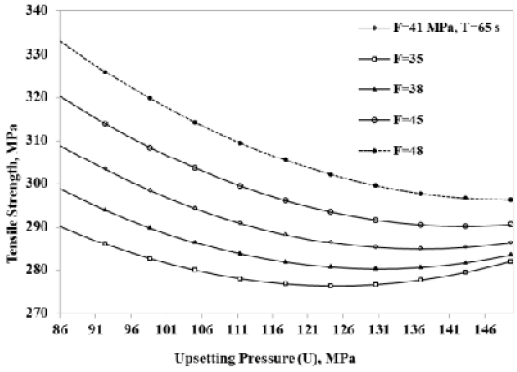

Fig. 7. Effect of upsetting pressure and friction pressure on tensile strength

Fig. 8 shows the interaction effects of friction time and upsetting pressure on flash diameter. All the curves show the same trend as friction time incresases. The flash diameter rapidly increases as friction pressure decreases. The friction welding flashes at the interface of joint are caused by a forge pressure and friction deformation, which is resulted in the heat zone or the plastic temperature range as demonstrated in paper [30].

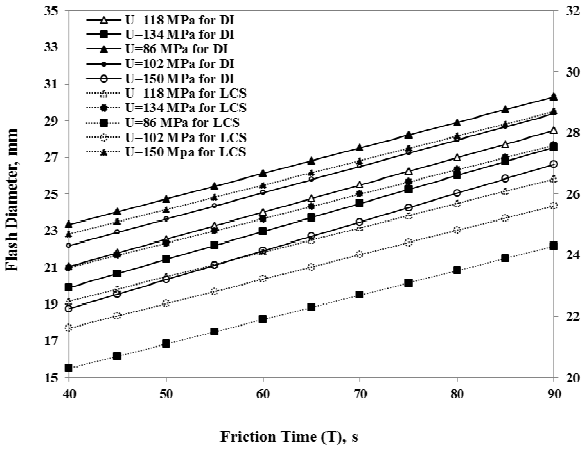

Fig. 8. Effect of upsetting pressure and friction pressure on tensile strength

5 Conclusions

The resulted model for the friction welding process explained 97% variance (R^2=0.97) for tensile strength, 99% variance (R^2=0.99) for ductile iron flash diameter and 94% (R^2=0.94) for low carbon steel flash diameter. The optimization was carried out using multi-objective genetic algorithm over the RSM model.

A maximum tensile strength of 392 MPa, minimum flash diameter of 17 and 24 mm for ductile iron and low carbon steel could be obtained under the welding conditions of friction pressure of 35 MPa, upsetting pressure of 150 MPa and friction time of 40 s.

Friction pressure and friction time have a positive effect on tensile strength. As friction pressure and friction time increases the tensile strength increases. However, initially the tensile strength decreases as friction time increase from 40 to 60s, reaches a minimum and then increases. The flash diameter and HAZ width also increase as friction time increases. Upsetting pressure has a negative effect on tensile strength. As upsetting pressure increases the tensile strength decreases.

Multi-objective optimization carried out with the RSM model using genetic algorithm approach generated a set of Pareto optimal points. Pareto front points (see Table 5) can aid the process operator to fix the input control variables.

References

1. N. Ozdemir, M Aksoy, N Orhan, J Mater Process Technol **14**, 228 (2003).
2. M. Ebrahimnia, F. Malek Ghaini, S.H. Gholizade, M. Salari, Mater Des **33**, 551(2012).
3. B. Crossland, Contemp Phys **12**, 559 (1971).
4. American Welding Society. Recommended practice for friction welding. Miami: AWS, (1989).
5. V.K. Lebedev, I.A. Chernenko. *Welding and surface reviews. Friction welding* (Harwood Academic Publishers, Amsterdam, 1992).
6. T. Shinoda, S. Endo, Y. Kato, Weld Int **13**, 89 (1991).
7. H. Richter, A. Palzkill, Schw. und Schn **11**,188 (1990).

8. R. Winiczenko, M. Kaczorowski, Mater. Des **34**, 444 (2012).
9. R. Winiczenko, M. Kaczorowski, J Mater. Process. Technol **213**, 453 (2013).
10. Ogara T, Kojoh K, Nagayoshi N, Jpn J Foundry Eng Soc **77**, 39 (2005).
11. AWS welding handbook. **2**. Miami: American Welding Society (1991).
12. ASM handbook. **6**. (ASM International, Materials Park, 1995).
13. S.B. Dunkerton, Weld J. **193**, (1986).
14. K. Deb. *Optimizations for engineering design–algorithm and examples* (Prentice Hall of India, New Delhi, 1996).
15. D.C. Montgomery. *Design and analysis of experiments* (Wiley, 2009).
16. R. Paventhan, Lakshminarayanan P.R, Balasubramanian V, J Iron. Steel. Res. Int **19**, 66 (2012).
17. R. Paventhan, P.R. Lakshminarayanan, V. Balasubramanian, Trans. of Nonf. Met. Soc. of China **21**, 1480 (2011).
18. P. Sathiya, S. Aravindan, A. H. Noorul, K. Paneerselvam, J Mater. Process. Technol **209**, 2576 (2009).
19. P. Sathiya, K. Panneerselvam, M.Y. Abdul Jaleel, Mater Des **32**, 1253 (2011).
20. H. Yamaguchi, K. Ogawa, K. Sakaguchi, J. Jpn. Inst. Light. Metal **41,** 716 (1991).
21. N. Ozdemir, F. Sarsirlmaz, A. Hascalik, Mater Des **28**, 301 (2007).
22. A. Hakan, T. Mehmet, K. Adem, Mater Des **28**, 948 (2007).
23. O. Koichi, Y. Hiroshi, K. Seiichi, S. Kazuhiko, J. Jpn. Weld. Soc **24,** 47 (1993).
24. T. Udayakumar, K. Raja, T.M Afsal Husain, P. Sathiya, Mater Des **53**, 226 (2014).
25. T. Udayakumar, K. Raja, A. Tanksale Abhijit, P. Sathiya, J Manuf Process **15**, 558 (2013).
26. *Design-Expert software version 8.0 user's* Guide (2009).
27. R.H. Myers, D.C. Montgomery, *Response surface methodology: process and product optimization using designed experiments* (New York, Wiley, 1995).
28. Y. Censor. Appl Math Optim **4**, 41 (1977).
29. D. Kalyanmoy. In: Chichester, editor. *Multi-objective optimization using evolutionary algorithms* (John Wiley and Sons, England, 2001).
30. J. Luo, Y.H. Ye, J.J. Xu, J.Y Luo, S.M. Chen, X.C Wang, Mater Des **30**, 353 (2009).